ISSN 0023-1584, Kinetics and Catalysis, 2017, Vol. 58, No. 1, pp. 81–91. © Pleiades Publishing, Ltd., 2017.
Original Russian Text © A.P. Savost'yanov, R.E. Yakovenko, G.B. Narochnyi, V.G. Bakun, S.I. Sulima, E.S. Yakuba, S.A. Mitchenko, 2017, published in Kinetika i Kataliz, 2017, Vol. 58, No. 1, pp. 86–97.

Industrial Catalyst for the Selective Fischer–Tropsch Synthesis of Long-Chain Hydrocarbons

A. P. Savost'yanov[a], R. E. Yakovenko[a], G. B. Narochnyi[a, *], V. G. Bakun[a], S. I. Sulima[a], E. S. Yakuba[a], and S. A. Mitchenko[a, b, **]

[a] *Platov South-Russian State Polytechnic University (NPI), Novocherkassk, Rostov oblast, 346128 Russia*
[b] *Litvinenko Institute of Physical Organic Chemistry and Coal Chemistry, National Academy of Sciences of Ukraine, Donetsk, 83114 Ukraine*
**e-mail: narochgb@bk.ru*
***e-mail: samit_RPt@mail.ru*
Received May 30, 2016

Abstract—The results of development of an industrial supported cobalt–silica gel catalyst for the Fischer–Tropsch synthesis are reported. The studies included the selection of a support and the determination of an optimum active component content, a calcination temperature, and the effect of doping with aluminum oxide on the physicochemical and catalytic properties of the $Co–SiO_2$ system. The catalyst samples were characterized by a set of physicochemical methods. The on-stream stability of the supported cobalt–silica gel catalyst was tested in the continuous mode for 1000 h. In the course of the entire test cycle, the catalyst exhibited stable operation under varied synthesis temperature and gas space velocity, and it can be recommended for industrial applications. The experimental results were used for the preparation of a pilot batch of the catalyst.

Keywords: Fischer–Tropsch synthesis, Co/SiO_2 catalyst, Al_2O_3 promoter, physicochemical properties, selectivity for C_{5+}

DOI: 10.1134/S0023158417010062

INTRODUCTION

The exhaustion of world oil reserves increases interest in technologies for the production of hydrocarbons from alternative sources (natural gas, associated petroleum gas, coal, peat, biomass, carbon-containing wastes, etc.), which can be converted into liquid motor fuel or raw materials for chemical and petrochemical industries [1]. Among them are the most promising technologies based on the conversion of carbon-containing matter into synthesis gas with the subsequent transformation of this latter into hydrocarbons by the Fischer–Tropsch (FT) process [2]. The synthetic hydrocarbons obtained by this process are in demand on the Russian and world markets. Thus, liquid hydrocarbons can be used as high-quality synthetic motor fuels (almost free from nitrogen, sulfur, and aromatic hydrocarbons) or for the production of reagents and standard reference substances, and α-olefins can be used as raw materials in the petrochemical branch of industry. Solid hydrocarbons (waxes) find use in the cosmetic, food, and defense branches of industry [3, 4], or they can be converted into liquid products by hydrocracking.

Industrial technology for the production of synthetic hydrocarbons according to this method was implemented at the plants of Sasol (at Sasolburg and Secunda in South Africa), Escravos (Nigeria), Shell (Bintulu, Malaysia, and Qatar), Sasol/QP (Ras Laffan, Qatar), and PetroSA (Mossel Bay, South Africa). Building of such plants is planned by ExxonMobil, Conoco, and Syntroleum [5, 6]. In Russia, a factory of this kind with an annual output of 50000 t occurred at the Novocherkassk plant of synthetic products (Rostov oblast). It was launched in 1952 with the use of technology, equipment, and catalyst developed in Germany. Subsequently, the German deposited cobalt–thorium (Co–Th) catalyst was replaced by an original cobalt–magnesium–zirconium (Co–Mg–Zr) catalyst [7, 8]. Initially, coal (anthracite) from the Donets Basin served as raw material; then, natural gas was used. In addition to gasoline and diesel fractions, the products of the plant included C_{35+} hydrocarbons (ceresin of brand 100) and individual high-purity hydrocarbons, including α-olefins with odd hydrocarbon numbers. This factory was in operation up to 1992, and it is currently lost.

It is obvious that these technologies should be renewed for the further development of the industry of synthetic hydrocarbons in the Russian Federation. The industrial production of synthetic hydrocarbons is planned to be implemented in Dzerzhinsk (Nizhny Novgorod oblast) [9, 10]; for this purpose, a pilot plant

for the synthesis of hydrocarbons from natural gas was preliminarily developed. The main engineering solutions used in this case were described elsewhere [11]. A new supported cobalt–silica gel catalyst whose production process was developed under industrial conditions [12] was proposed as a catalyst for the synthesis of long-chain hydrocarbons.

Here, we report the studies performed in the development of a commercial cobalt–silica gel (Co/SiO_2) catalyst with an increased selectivity for C_{35+} hydrocarbons.

EXPERIMENTAL

Catalyst Preparation

The catalyst samples were prepared by the impregnation of a support with an aqueous solution of cobalt nitrate in a single step. Commercial KSKG silica gel (*GOST* [State Standard] *3956-76*, Salavat Catalyst Factory, Russia) was used as the support. The concentration of cobalt nitrate in the impregnating solution was varied in a range of 20–55 wt %. The support was impregnated at a temperature of 80°C for 0.5 h. The catalyst was dried under the following conditions: at 80°C for 6 h and at 100, 120, and 140°C for 2 h at each particular temperature; then, it was calcined at 400°C for 4 h. The effect of final heat treatment regimes on the properties of catalysts was studied with the samples calcined at final temperatures of 200, 250, 300, 400, and 500°C. It was preliminarily found that an optimum rate of sample heating is 5 K/min. The cobalt content of all of the catalyst samples with different calcination temperatures was 20 ± 0.5 wt %.

For the determination of the effect of an Al_2O_3 additive on the properties of cobalt–silica gel catalysts, aluminum was introduced in the form of nitrate together with cobalt nitrate at the stage of impregnation. The catalyst samples were designated as Co–$x$$Al_2O_3/SiO_2$, where x = 0.4, 1, 2, and 3 wt % is the aluminum oxide content of the catalyst. The cobalt content of the test catalyst samples was varied in a range of 20.9–22.8 wt %.

Characterization of Physicochemical Properties

The cobalt content was determined by X-ray fluorescence elemental analysis (XRFEA) on an ARL QUANT'X EDXRF X-ray spectrometer (Thermo Electron Corporation, United States) in an atmosphere of air with the use of a Teflon substrate with an effective irradiation area of 48.99 mm^2.

The X-ray diffraction (XRD) analysis of the calcined catalysts was carried out on an ARL X'TRA powder diffractometer (Thermo Fisher Scientific, United States) with monochromatic CuK_α radiation by point-by-point scanning (step size, 0.01°; counting time per data point, 2 s) in the 2θ range from 15° to 70°. Qualitative phase composition was determined with the aid of the PDF-2 database [13] and the Crystallographica software. Crystallite sizes were calculated from the Scherrer equation [14].

The studies of the catalysts by temperature-programmed reduction (TPR) were carried out on a ChemiSorb 2750 chemisorption analyzer (Micromeritics, United States) with a thermal conductivity detector. The sample (0.1–0.2 g) was preliminarily kept in a flow of helium (20 mL/min) at a temperature of 200°C for 2 h; then, it was cooled to 20°C, blown with a mixture of 10% H_2 in nitrogen (20 mL/min), and reduced in a temperature range of 20–800°C at a rate of 5 K/min.

The ChemiSorb 2750 analyzer (Micromeritics) with a thermal conductivity detector was used for the study of catalysts by the temperature-programmed desorption of CO (CO TPD). The catalyst sample was reduced in accordance with the above procedure. The pulse adsorption of CO until sample surface saturation was performed in a flow of helium (20 mL/min), and physically adsorbed gas was removed by blowing for 1 h at 100°C. CO was desorbed by increasing the temperature from 25 to 800°C at a rate of 20 K/min.

The micrographs of catalysts were obtained on a Tecnai G2 Spirit BioTWIN transmission electron microscope (FEI, United States) at an accelerating voltage of 120 kV. The samples of the reduced catalysts were ground in a flow of CO_2 and supported on copper grids as suspensions in toluene.

Catalytic Tests

The Fischer–Tropsch synthesis was carried out in a steel flow reactor (inside diameter, 28 mm) with a fixed catalyst bed (70 cm^3) at atmospheric or elevated pressure (1.5 MPa). The catalyst samples were preliminarily reduced in a flow of hydrogen (GHSV = 1000 h^{-1}) at 400°C for 1 h.

Before the catalytic tests, all of the catalysts were activated at GHSV = 100 h^{-1} in synthesis gas containing 33 vol % CO and 67 vol % H_2. The activation was carried out under a pressure of 0.1 MPa with a stepwise increase in the temperature (2.5 K/h) from 150°C to a temperature at which ~50% CO conversion was reached. Then, the temperature was decreased to 160°C and the specified values of pressure and gas space velocity were adjusted; the temperature was increased once again to the specified value at a rate of 2.5 K/h. After catalyst activation with synthesis gas, the synthesis products were removed from collectors and a balance experiment was performed for 90–120 h.

The activity of the catalyst samples with different active component contents and final heat treatment temperatures was determined at GHSV = 100 h^{-1} and a pressure of 0.1 MPa.

The effect of the Al_2O_3 promoter on the properties of cobalt–silica gel catalysts was studied in a synthesis

temperature range of 213–220°C at GHSV = 1000 h^{-1} and a pressure of 2.0 MPa.

The on-stream stability tests of the Co–1%Al_2O_3/SiO_2 catalyst were conducted at a pressure of 1.5 MPa with the use of synthesis gas containing 20 vol % CO, 40 vol % H_2, and 40 vol % N_2.

The composition of the synthesis gas and gaseous synthesis products was analyzed by gas-adsorption chromatography on a Kristall 5000 chromatograph (Khromatek, Russia) with a thermal conductivity detector and two columns. The first Haysep R column was used for the analysis of C_1–C_5 hydrocarbons and CO_2 (carrier gas, helium; flow rate, 15 mL/min), and the second column (molecular sieve NaX) was used for the determination of CO, H_2, and N_2 (carrier gas, argon; flow rate, 15 mL/min). Temperature-programmed conditions (80–240°C; heating rate, 8 K/min) were used.

The composition of C_{5+} hydrocarbons was determined by capillary gas chromatography–mass spectrometry on an Agilent GC 7890 gas chromatograph (Agilent, United States) equipped with an MSD 5975C mass-selective detector and an HP-5MS capillary column.

RESULTS AND DISCUSSION

Selection of a Support and Determination of the Optimum Cobalt Content

The technology of supported cobalt-containing catalysts differs from that of precipitated ones in a number of advantages: the simplicity of technological operations, the possibility of active component regeneration, and a smaller amount of waste [15]. The main function of supports in catalysts, including those in the FT process, is to afford a high dispersity and specific surface area of the supported active metal [16]. The support should have a developed polymodal porous structure and a large and accessible specific surface area [17]. On the supporting of an active component, it can interact with the support and form new compounds and phases [18]. The support frequently manifests independent activity in the course of synthesis to catalyze the subsequent transformations of the initial products of the FT synthesis; this is characteristic of zeolites [19–21].

The following commercially available supports were studied previously [10, 11]: silica gel, synthetic aluminosilicate, and aluminum oxides of different grades. It was found that the Co/SiO_2 catalytic system is promising for the synthesis of long-chain hydrocarbons. In order to determine the effect of the active component content on the catalytic properties of a supported Co/SiO_2 catalyst and an optimum catalyst composition, we prepared samples with different cobalt contents of 8.5–22.0 wt %. We found that the dependence of the cobalt content of the supported catalyst on cobalt nitrate concentration in the impregnating solution (Fig. 1) is described by the following equation (correlation coefficient, 0.99):

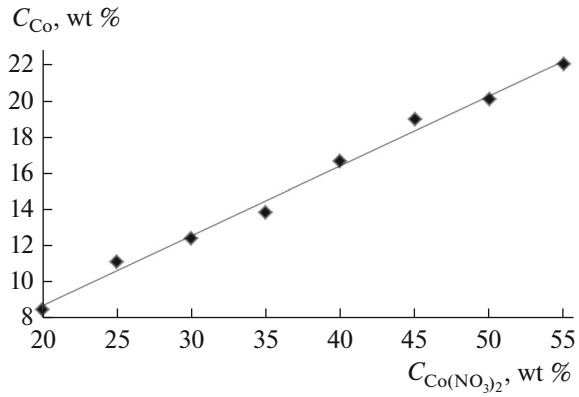

Fig. 1. Dependence of the cobalt content (C_{Co}) of the catalyst on the cobalt nitrate concentration ($C_{Co(NO_3)_2}$) in the impregnating solution.

$$C_{Co} = 0.39C_{Co(NO_3)_2} + 1.06,$$

where C_{Co} is the cobalt content of the catalyst (wt %), and $C_{Co(NO_3)_2}$ is the cobalt nitrate concentration in the impregnating solution (wt %). This equation is correct in the range of cobalt concentrations of 8.0–22.0 wt % in the catalyst.

With increasing the cobalt content of the Co/SiO_2 catalyst, the yield of C_{5+} hydrocarbons increased (Fig. 2) and reached a maximum at a cobalt content of ~20.0 wt %. A further increase in the cobalt content of the catalyst led to a decrease in selectivity and productivity. It is obvious that the above decrease in productivity with respect to the C_{5+} hydrocarbons is related to a decrease in the dispersity of the active component [2, 22].

Thus, the optimum cobalt content of the catalyst on the KSKG support is ~20.0 wt %.

Effect of the Thermal Pretreatment of a Catalyst on Its Activity and Selectivity in the FT Synthesis

It is well known [23] that the optimum size of cobalt crystallites in a reduced form on the support surface should be 6–8 nm. The rate of heating and the final calcination temperature at the stage of the preparation of the oxide form of the catalyst exert a considerable effect on the dispersity of active component particles [24]. At a high rate of thermal treatment, the active component is comparatively evenly distributed over the support surface: in this case, rapid evaporation excludes the entering of new solution portions because of capillary flow or film transfer. On the contrary, comparatively coarse particles are formed at a low rate of heating (because of the gradual additional supply of new

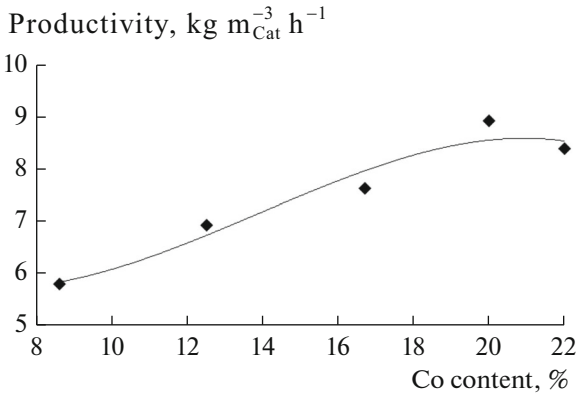

Fig. 2. Effect of the cobalt content of the Co/SiO_2 catalyst on the productivity for C_{5+} hydrocarbons.

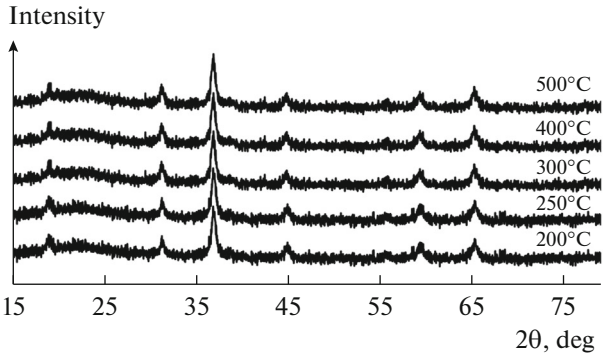

Fig. 3. X-ray diffraction patterns of the Co/SiO_2 catalyst samples with different final calcination temperatures.

solution portions to the supported cobalt particles formed) [25].

The experimental results (Table 1) are consistent with the above concepts. The samples calcined at low final temperatures of 200 and 250°C exhibited lower activity in the FT synthesis. Thus, the CO conversion on the Co/SiO_2 catalyst (200°C) at a temperature of 190°C and on Co/SiO_2 (250°C) at 195°C was 48.8 and only 45.8%, respectively. As the synthesis temperature was increased, the increased formation of gases (C_1–C_4) was observed; as a consequence, selectivity for C_{5+} hydrocarbons decreased. The calcination of catalyst samples in a range of 300–500°C increased their catalytic activity: the CO conversion on these samples was higher than 50% even at 180°C. Selectivity for the C_{5+} hydrocarbons was also higher on the catalysts calcined at a temperature of 400–500°C. This fact is indicative of the formation a larger number of polymerization sites on the surface of these catalytic systems.

The samples with different calcination temperatures were studied by XRD analysis and TPR. The XRD analysis of Co/SiO_2 catalyst samples in oxide form showed that all of the samples exhibited diffraction patterns of the same type (Fig. 3): SiO_2 was X-ray amorphous, and cobalt occurred in the structure of catalysts in the form of a number of reflections from the crystalline phase of the Co_3O_4 oxide. The sizes of the Co_3O_4 crystallites estimated from the Scherrer equation were in a range of 13–16 nm.

Figure 4 shows the results of the TPR studies. The spectra of the Co/SiO_2 catalyst samples with final calcination temperatures of 200, 250, and 300°C exhibited weak peaks in a range of 150–200°C, which can be attributed to the reductive decomposition of residual cobalt nitrate. These peaks are absent from the spectra of the Co/SiO_2 (400°C) and Co/SiO_2 (500°C) samples; this fact indicates the almost complete decomposition of cobalt nitrate at final treatment temperatures of 400 and 500°C. In addition to the low-temperature peak noted, two intense reduction peaks were present in a range of 280–650°C with maximums at 300–330 and 370–470°C, which will be referred to as signal 1 and signal 2, respectively (Table 2). These peaks of hydrogen absorption can be attributed to the stepwise reduction of a Co_3O_4 cobalt oxide phase [26, 27] according to the following reaction equations:

$$Co_3O_4 + H_2 \rightarrow 3CoO + H_2O, \quad \text{(I)}$$

$$CoO + H_2 \rightarrow Co^0 + H_2O. \quad \text{(II)}$$

Table 1. Catalytic properties of Co/SiO_2 catalyst samples with different final calcination temperatures

Calcination temperature, °C	Synthesis temperature, °C	CO conversion, %	Selectivity, %			
			CH_4	C_2–C_4	C_{5+}	CO_2
200	190	48.8	14.5	14.5	69.5	1.5
250	195	45.8	16.8	18.0	63.6	1.6
300	180	52.1	7.5	7.1	83.8	1.6
400	180	52.2	5.2	5.6	88.7	1.5
500	180	52.5	5.4	5.4	87.0	2.2

The S_1/S_2 ratio between the areas of signals 1 and 2 increased with catalyst calcination temperature (Table 2) to approach a value of 3, which is theoretically expected from the stoichiometry of cobalt oxide reduction (Eqs. (I) and (II)). Obviously, the smaller values of the S_1/S_2 ratio for the samples with final calcination temperatures lower than 400°C can be attributed to the partial oxidation of cobalt at low calcination temperatures.

The calcination temperature has an essential effect on the physicochemical and catalytic properties of supported catalysts; for the catalyst developed, it should be in a range of 400–500°C, which is consistent with published data [28].

Effect of the Al_2O_3 Promoter on the Properties of Cobalt–Silica Gel Catalysts

Promotion with noble metals [2, 29–32] substantially facilitates the reduction of cobalt and increases the productivity of catalysts. In spite of the strong promoting effect of noble metals on catalysts for the FT synthesis, the industrial application of these metals is limited because of their high cost [32, 33]. The doping of cobalt catalysts with inexpensive and readily available promoters such as metal oxides is a more acceptable method for improving the properties of FT catalysts [2, 34, 35]. Recently, Zhang et al. [36] reported that the introduction of aluminum oxide into a 10 wt % Co/SiO_2 catalyst considerably increased activity and selectivity for C_{5+} hydrocarbons in the FT synthesis in a slurry reactor at 240°C and a pressure of 1 MPa. Pei et al. [37] obtained similar results in the FT synthesis at 220°C and 3 MPa in a tubular fixed-bed reactor with the 15 wt % Co/activated carbon catalyst. They carried out the reactions on a laboratory scale with a relatively short time of catalyst testing (to 24 h) [37]. In this work, we studied the effects of promotion with aluminum oxide in prolonged catalytic experiments (150 h) at a pilot plant, which simulated the conditions of the industrial FT synthesis.

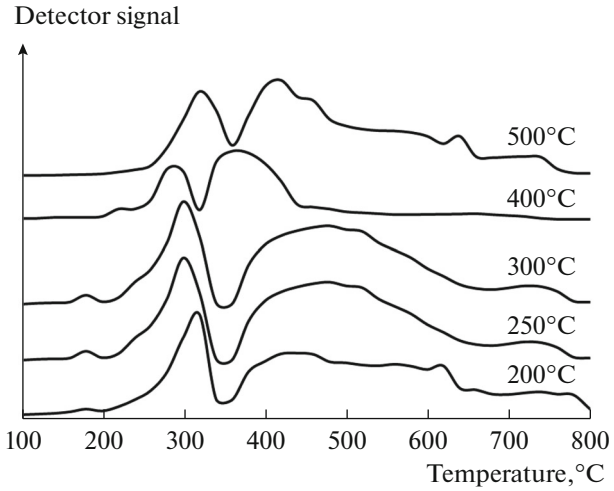

Fig. 4. TPR spectra of the Co/SiO_2 catalyst samples with different final calcination temperatures.

Table 3 summarizes the catalytic characteristics of cobalt–silica gel catalyst samples promoted with aluminum oxide in the FT synthesis over a temperature range of 213–220°C. The characteristics were measured at a pressure of 2.0 MPa and a gas space velocity of 1000 h^{-1} because, under the conditions of the intense FT process, the promoting effect of the introduction of Al_2O_3 became more pronounced: the formation of CH_4 decreased by a third; the conversion of CO increased, and the productivity of catalysts with respect to a C_{5+} fraction also increased by 5–13% with an increase in the aluminum oxide content to 1 wt %.

Table 4 shows the effect of aluminum oxide additives to the Co/SiO_2 catalyst on the distribution of C_{5+} products. Alkanes are the main products obtained on all of the catalysts. Olefins and alcohols were also formed in trace amounts on the catalyst not promoted with aluminum oxide. The low yields of these products increased by a factor of almost two on the catalyst with an optimum 1 wt % content of aluminum oxide, and they increased considerably as the

Table 2. TPR spectra of the catalyst samples depending on calcination temperature

Calcination temperature, °C	Signal 1		Signal 2		S_1/S_2
	maximum, °C	area S_1, %	maximum, °C	area S_2, %	
200	303	28	474	72	2.5
250	317	30	440	70	2.4
300	318	27	430	73	2.7
400	295	26	370	74	2.9
500	328	26	416	74	2.9

Table 3. Catalytic properties of the promoted $Co–xAl_2O_3/SiO_2$ catalysts

Catalyst	CO conversion, %	Selectivity, %				Productivity with respect to C_{5+} hydrocarbons, kg m^{-3} h^{-1}
		CH_4	$C_2–C_4$	C_{5+}	CO_2	
Co/SiO_2	49.0	15.4	6.6	77.4	0.6	90.4
$Co–0.4Al_2O_3/SiO_2$	51.1	10.8	9.3	79.5	0.4	95.0
$Co–1Al_2O_3/SiO_2$	53.9	10.7	8.4	80.1	0.7	102.4
$Co–2Al_2O_3/SiO_2$	46.2	17.6	7.7	74.2	0.6	79.5
$Co–3Al_2O_3/SiO_2$	22.7	23.5	13.7	62.0	0.8	33.2

Table 4. Proportions of C_{5+} products of the FT synthesis over the $Co–xAl_2O_3/SiO_2$ catalysts

Al_2O_3 content, wt %	Product distribution, wt %				
	paraffins			olefins	alcohols
	$C_5–C_{18}$	$C_{19}–C_{35}$	C_{35+}	$C_5–C_{18}$	$C_5–C_{18}$
0	49.6	47.6	2.4	0.4	0.04
1.0	54.9	42.1	2.3	0.7	0.07
3.0	48.1	37.5	2.2	10.1	1.2

Table 5. Average size (d) of the Co^0 nanoparticles in the reduced $Co–xAl_2O_3/SiO_2$ catalysts

x, wt %	d, nm
0	12 ± 2
0.4	8 ± 2
1.0	8 ± 2
2.0	11 ± 2

amount of Al_2O_3 was further increased. Figure 5 shows the histograms of the molecular-weight distributions of C_{5+} paraffins. The promotion of the catalysts with aluminum oxide (1 wt %) changed the molecular-weight distribution to make it narrower due to an increase in the fraction of $C_8–C_{25}$.

Thus, the doping of Co/SiO_2 with aluminum oxide exerted a promoting effect on the catalytic activity and selectivity of the FT synthesis. Under the test conditions, the greatest promoting effect was observed in catalyst samples with aluminum oxide additives to 1 wt %. A further increase in the aluminum oxide content led to an opposite effect.

Promotion with Al_2O_3 did almost not change the texture of catalysts, which is caused by the nature of the support (the specific surface area was 230–239 m^2/g, and the mean pore diameter and the total pore volume were 8–11 nm and 0.6–0.7 cm^3/g, respectively); however, it substantially changed the particle size of the active component. The size distribution of cobalt crystallites for reduced catalysts with different concentrations of Al_2O_3 additives were studied by TEM (Fig. 6). An increase in the aluminum oxide content to 1.0 wt % facilitated a decrease in the particle sizes of cobalt (an increase in the dispersity) and a narrowing of particle-size distribution. A further increase in the concentration of the promoter to 2.0 wt % led to a coarsening of Co nanoparticles and a broadening of the particle-size distribution. Table 5 summarizes the average sizes of Co^0 nanoparticles.

It is believed that the Al_2O_3 additives in a specific amount inhibit the aggregation of cobalt metal nanoparticles; this manifests itself in a decrease in the average particle size. The total number of active cobalt atoms on the external surface of the nanoparticles increases with the dispersity of Co^0; because of this, the catalyst activity in the FT synthesis increases. The above effect of the average size of cobalt nanoparticles on the selectivity of the FT synthesis on Co/SiO_2 can also be a consequence of the activity of the cobalt nanoparticles in the hydrogenolysis of the hydrocarbons formed. Recently, Peng et al. [38] found that high activity in the selective hydrogenolysis of hexadecane to lighter hydrocarbons ($C_{10}–C_{15}$) under the Fischer–Tropsch synthesis conditions was observed on cobalt catalysts with the average size of cobalt nanoparticles of precisely 8 nm. Therefore, it is possible to assume that the more intensive subsequent hydrogenolysis of long-chain hydrocarbons on the Co^0 nanoparticles is responsible for the observed increase in the fraction of $C_8–C_{25}$ hydrocarbons due to heavier products (Fig. 5)

in the FT synthesis on the $Co–1Al_2O_3/SiO_2$ catalyst, as compared with that on Co/SiO_2.

On the other hand, the doping of Co/SiO_2 with aluminum oxide can create a certain acidity of the support [39]; therefore, the possibility of acid catalysis in the hydrogenolysis of the resulting hydrocarbons cannot be excluded [38, 40]. In particular, the observed sharp increase in selectivity for CH_4 and olefins on the $Co–3Al_2O_3/SiO_2$ catalyst, as compared with that on $Co–1Al_2O_3/SiO_2$ (Table 1), can be a consequence of the expected higher concentration of acid sites on the surface of the former catalyst and the consecutive demethylation of hydrocarbons on them.

For studying the effect of the aluminum oxide content on the adsorption of CO on the reduced catalysts, we used the CO TPD method. Figure 7 shows the CO TPD profiles for the reduced $Co–xAl_2O_3/SiO_2$ samples. A hardly distinguishable desorption peak at ~70°C can be attributed to physically adsorbed CO. In addition to this low-intensity peak, two main desorption signals were present: a low-temperature peak with a maximum at ~220°C, which can be attributed to the desorption of chemisorbed CO, and a high-temperature peak with a maximum at ~750°C, which can be attributed to the desorption of CO_2 formed from the chemisorbed CO according to the Boudoir reaction.

The addition of aluminum oxide did not change the position of the low-temperature peak. At the same time, the area of the low-temperature signal monotonically increased as the Al_2O_3 content was increased to 1 wt % (Table 6). However, a further increase in the Al_2O_3 load over 1 wt % produced an opposite effect: the low-temperature signal area decreased. Obviously, this dependence of the chemisorption of CO on the introduced amount of aluminum oxide with a maximum to 1 wt % is a consequence of the maximum dispersity of cobalt metal, which is reached exactly at this amount of Al_2O_3 added.

Note that, in addition to the above structure factors, electronic effects can also play a specific role. It is well known that aluminum oxide possesses electron-donor properties [36]. The presence of donor particles on the catalyst surface will facilitate the adsorption of CO because carbon monoxide is a π acceptor. Then, aluminum oxide can be considered not only as a structural promoter, which leads to an increase in the dispersity of cobalt, but also as an electronic promoter, which modifies the chemisorption properties of the active metal. Both of these functions of aluminum oxide enhance the adsorption of CO. On the other hand, Zhang et al. [36] demonstrated that Al_2O_3 as a promoter inhibits the adsorption of H_2; this also leads to a decrease in the H_2/CO ratio on the surface of the promoted catalysts.

It is necessary to emphasize that the H_2/CO ratio between the surface concentrations of adsorbed gases was related [25, 28, 38] to the selectivity and distribution of products in the FT synthesis. Peng et al. [38] assumed that the predominance of superficially adsorbed hydrogen leads to an increase in the process of CO hydrogenation and, correspondingly, in selectivity for methane. Conversely, a higher concentration of CO on the surface facilitates the growth of a carbon chain with the formation of longer chain products. It is likely that these effects can explain better selectivity for the C_{5+} hydrocarbons on the Co/SiO_2 catalysts promoted with aluminum oxide.

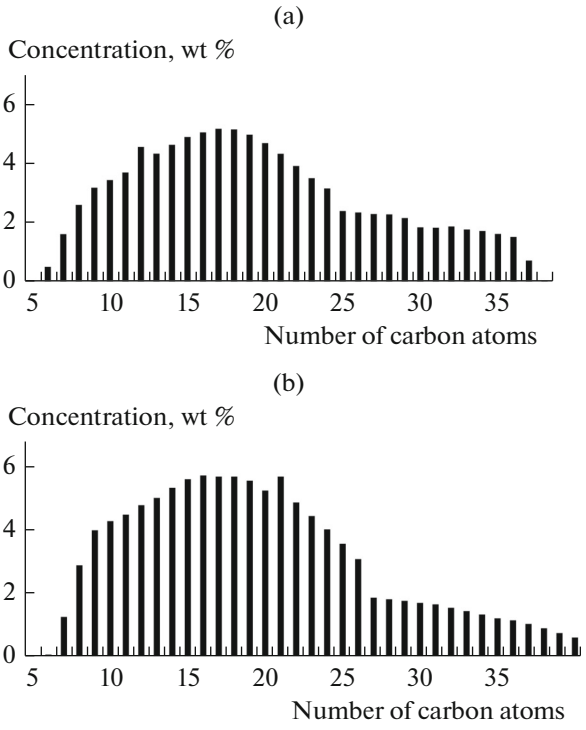

Fig. 5. Molecular-weight distributions of the C_{5+} paraffins obtained on the (a) Co/SiO_2 and (b) $Co–1Al_2O_3/SiO_2$ catalysts.

On-Stream Stability of the $Co–Al_2O_3/SiO_2$ Catalyst

For the industrial use of the supported cobalt–silica gel catalyst, it was necessary to estimate the stability of its operation in the continuous mode under

Table 6. Characteristics of the low-temperature peak of CO TPD for the reduced catalysts

Catalyst	T_{max}, °C	Area, %
Co/SiO_2	207	12
$Co–0.4Al_2O_3/SiO_2$	207	15
$Co–1Al_2O_3/SiO_2$	220	18
$Co–2Al_2O_3/SiO_2$	219	8
$Co–3Al_2O_3/SiO_2$	221	7

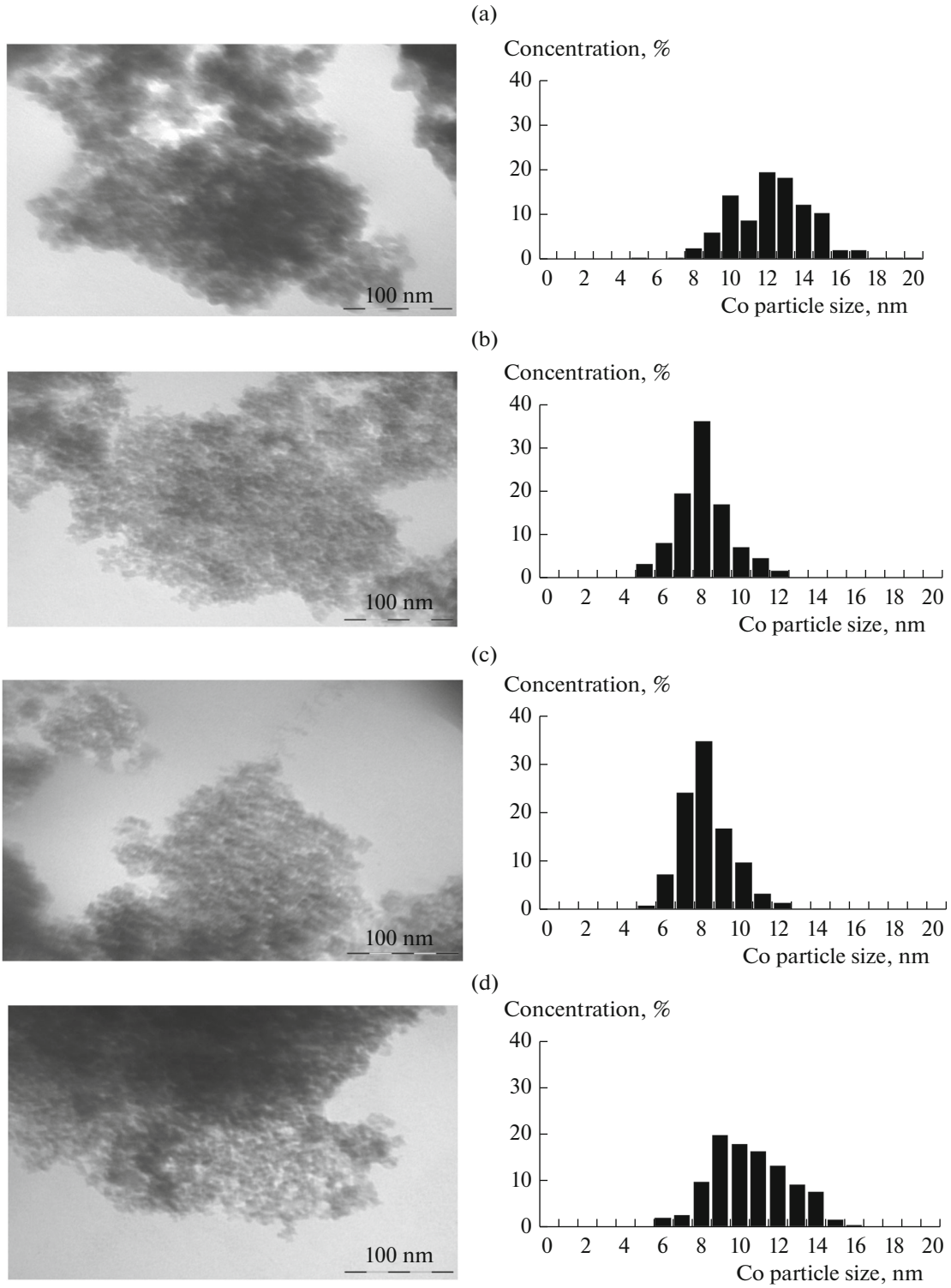

Fig. 6. TEM images of the reduced catalysts and cobalt particle size distribution histograms: (a) Co/SiO_2, (b) $Co–0.4Al_2O_3/SiO_2$, (c) $Co–1Al_2O_3/SiO_2$, and (d) $Co–2Al_2O_3/SiO_2$.

long-term service conditions. The process parameters (temperature, gas space velocity, etc.) can be changed under industrial conditions, and this can affect the catalytic properties of the catalyst.

The on-stream stability of the cobalt–silica gel catalyst was studied at a pressure of 1.5 MPa in a flow system in the continuous mode for 1000 h in cycles (Table 7). The results of the studies were represented

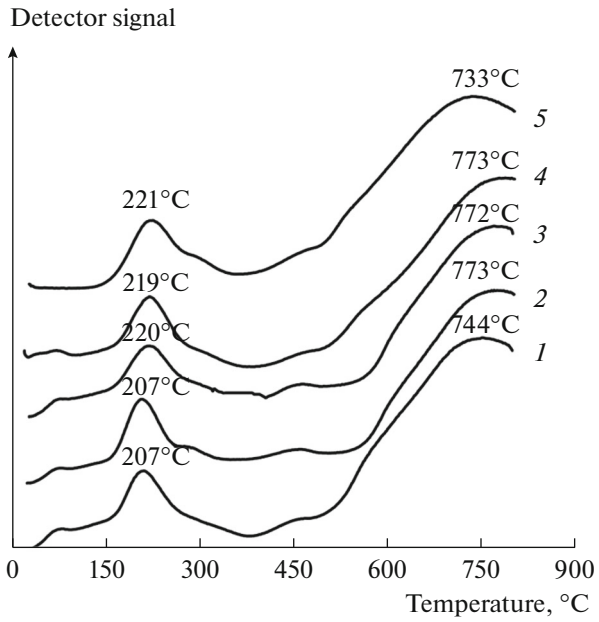

Fig. 7. CO TPD spectra of the reduced catalysts: (*1*) Co/SiO_2, (*2*) $Co–0.4Al_2O_3/SiO_2$, (*3*) $Co–1Al_2O_3/SiO_2$, (*4*) $Co–2Al_2O_3/SiO_2$, and (*5*) $Co–3Al_2O_3/SiO_2$.

as a diagram of CO conversion (x_{CO})–synthesis temperature (T)–catalyst on-stream time (τ) (Fig. 8).

In the initial period of tests (first cycle, Fig. 8), ~52% CO conversion was reached at a gas space velocity (GHSV) of 100 h^{-1} and a temperature of 170°C; the conversion decreased to 45% after 30 h of continuous catalyst operation and remained almost unchanged during the entire period of the first cycle. Table 8 summarizes the group and fractional compositions of the condensed hydrocarbons obtained in the first cycle. Long-chain (C_{19+}) unbranched saturated hydrocarbons were predominantly formed.

In the second cycle, the gas space velocity and temperature were decreased (to 60 h^{-1} and 165°C, respectively). The CO conversion changed only slightly in the course of this cycle, and it varied over a range of 55–60%. In the third cycle of tests, the temperature was elevated to 183°C at a constant gas space velocity (60 h^{-1}) in order to increase the CO conversion. In the course of this cycle, the conversion of CO was 71–72%.

In the fourth cycle of tests, the gas space velocity was increased to 100 h^{-1} at a fixed temperature; this led to a small increase in the conversion of CO (to 76%) at the beginning of work, whereas these values reached a steady level of 72–73% at the end of the cycle. In the fifth cycle of tests, we returned to the conditions of the first cycle (GHSV = 100 h^{-1}, 170°C). After 30 h of operation in this mode, the CO conversion asymptotically approached a value of 46%, which coincided with the CO conversion in the first cycle. At the final sixth stage of the studies, the conversion of CO was increased to 55% due to an increase in the temperature to 175°C. In the first 200 h of continuous catalyst operation, the conversion monotonically decreased from 55 to ~48% and then remained almost unchanged within the next 350 h of operation.

As follows from the data given in Table 9, the catalyst that operated for a significant time under the conditions of varied gas space velocity and synthesis temperature exhibited stable catalytic properties. Selectivity for C_{5+} hydrocarbons, including long-chain C_{35+} hydrocarbons, and the fractional composition of the resulting hydrocarbons did not substantially change. The molecular-weight distribution of hydrocarbons corresponded to a chain growth probability (α) of 0.94.

Thus, the $Co–1Al_2O_3/SiO_2$ catalyst exhibited stable operation under varied FT process parameters for 1000 h of the entire period of tests; this fact evidences that it is promising for applications in industrial technologies.

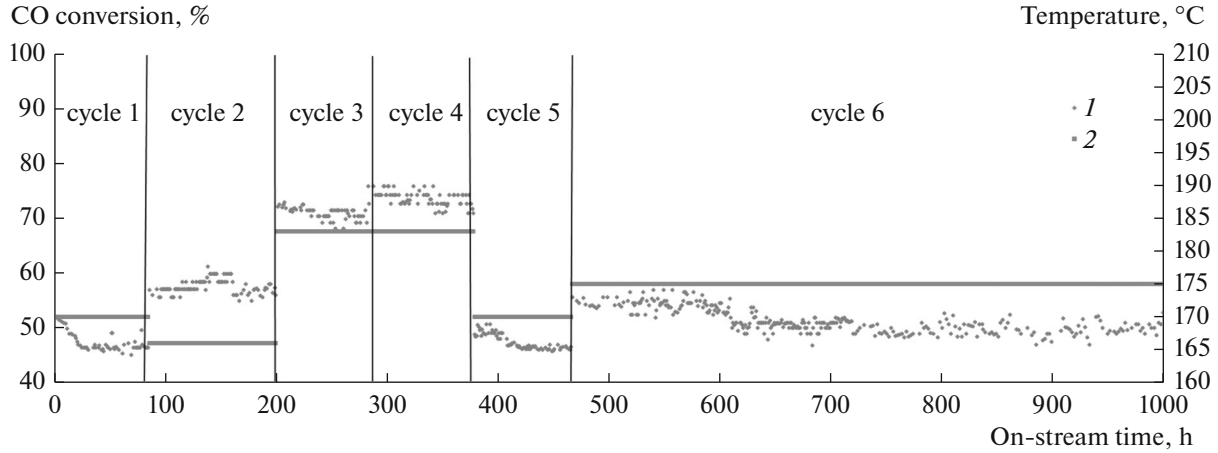

Fig. 8. The $x_{CO}–T–\tau$ time diagram obtained by experimental testing of the supported cobalt–silica gel catalyst: (*1*) CO conversion and (*2*) temperature.

Table 7. Operation cycles of the Co–$1Al_2O_3/SiO_2$ catalyst at 1.5 MPa

Cycle	GHSV, h^{-1}	Temperature, °C	On-stream time, h
First	100	170	80
Second	60	165	120
Third	60	183	80
Fourth	100	183	100
Fifth	100	170	80
Sixth	100	175	540

Table 8. Group and fractional compositions of the hydrocarbons synthesized in the first cycle

Group composition	Fractional composition, wt %		
	C_5–C_{10}	C_{11}–C_{18}	C_{19+}
n-Alkanes	8.9	31.8	57.7
Isoalkanes	0.1	0.2	0.1
Alkenes	0.7	0.5	0.0
Total	9.7	32.5	57.8

Table 9. Catalytic properties of the Co–$1Al_2O_3/SiO_2$ catalyst in the first and sixth cycles

Temperature, °C	CO conversion, %	Selectivity, %			Fractional composition, wt %		
		CH_4	C_{5+}	C_{35+}	C_5–C_{10}	C_{11}–C_{18}	C_{19+}
170	45	4.7	89.0	33.1	9.7	32.5	57.8
175	48	5.2	88.4	31.8	11.5	33.6	54.9

CONCLUSIONS

The set of studies on the development of a cobalt-containing supported catalyst for the selective synthesis of long-chain hydrocarbons on an industrial scale allowed us to make the following conclusions:

(1) We found that KSKG silica gel is an effective support for the cobalt-containing catalyst for the synthesis of hydrocarbons with an optimum cobalt content of 20.0 wt %.

(2) We found that the maximum productivity and selectivity for C_{35+} hydrocarbons were reached upon catalyst calcination at a temperature of 400–500°C at the stage of the preparation of the oxide form.

(3) We observed a considerable promoting effect of aluminum oxide in an amount to 1 wt % on the size of cobalt crystallites and, as a consequence, on the activity and selectivity of the catalyst.

(4) We tested the on-stream stability of the Co–$1Al_2O_3/SiO_2$ catalytic system at a pilot plant for 1000 h of continuous operation; this made it possible to obtain long-chain hydrocarbons with a chain growth probability of 0.94.

ACKNOWLEDGMENTS

This work was supported by the Russian Science Foundation (project no. 14-23-00078) and was performed with the use of laboratory equipment of the Nanotechnology Shared Facilities at the Platov South-Russian State Polytechnic University (NPI).

REFERENCES

1. David, A., Wood, A., and Chikezie, N., *J. Nat. Gas Sci. Eng.,* 2012, vol. 9, p. 196.
2. Khodakov, A.Y., Chu, W., and Fongarland, P., *Chem. Rev.,* 2007, vol. 107, p. 1692.
3. Bekker, M., Louw, N.R., Rensburg, J.V., and Potgiete, J., *Int. J. Cosmet. Sci.,* 2013, vol. 35, p. 99.
4. www.sasolwax.com/paraffin_wax.html. Accessed August 29, 2016.
5. Mordkovich, V.Z., Sineva, L.V., Kul'chakovskaya, E.V., and Asalieva, E.Yu., *Katal. Prom–sti.,* 2015, no. 5, p. 23.
6. Ellepola, J., Thijssen, N., Grievink, J., Baak, G., Avhale, A., and Schijndel, J.V., *Comput. Chem. Eng.,* 2012, vol. 42, p. 2.
7. Krylova, A.Yu. and Kozyukov, E.A., *Solid Fuel Chem.,* 2007, vol. 41, no. 6, p. 335.
8. Grigor'ev, D.A., *Neft', Gaz Biznes,* 2011, no. 3, p. 51.
9. Savost'yanov, A.P., Narochnyi, G.B., Yakovenko, R.E., Bakun, V.G., and Zemlyakov, N.D., *Catal. Ind.,* 2014, vol. 6, no. 4, p. 292.
10. Yakovenko, R.E. and Narochnyi, G.B., Bakun. V.G., Astakhov A.V., *Izv. Vyssh. Uchebn. Zaved,. Severo-Kavkazskii Region, Tekh. Nauki,* 2014, no. 6, p. 92.
11. Savost'yanov, A.P., Narochnyi, G.B., Yakovenko, R.E., Astakhov, A.V., Zemlyakov, N.D., Merkin, A.A., and Komarov, A.A., *Catal. Ind.,* 2014, vol. 6, no. 3, p. 212.
12. Narochnyi, G.B., Yakovenko, R.E., Savost'yanov, A.P., and Bakun, V.G., *Catal. Ind.,* 2016, vol. 8, no. 2, p. 139.
13. PDF-2, The Powder Diffraction File, International Center for Diffraction Data (ICCD), PDF-2 Release 2012. http://www.icdd.com.
14. *The Rietveld Method,* Young, R.A., Ed., Oxford: Oxford Univ. Press, 1995.
15. Satterfield, C., *Heterogeneous Catalysis in Practice,* New York: McGraw-Hill, 1980.
16. Boreskov, G.K., *Geterogennyi kataliz* (Heterogeneous Catalysis), Moscow: Nauka, 1986.
17. Krylov, O.V., *Geterogennyi kataliz* (Heterogeneous Catalysis), Moscow: Akademkniga, 2004.

18. Slivinskii, E.V., Kliger, G.A., Kuz'min, A.E., Abramova, A.V., and Kulikova, E.A., *Ross. Khim. Zh.,* 2003, vol. 47, no. 6, p. 12.
19. Kibby, C., *Catal. Today,* 2013, vol. 215, p. 131.
20. Sun, J., *Catal. Sci. Technol.,* 2014, vol. 4, p. 1260.
21. Yao, M., *Catal. Sci. Technol.,* 2015, vol. 5, p. 2821.
22. Girardon, J.S., *J. Catal.,* 2005, vol. 230, p. 339.
23. Chernavskii, P.A., Chu, Vei., Khodakov, A.Yu., Pankina, G.V., and Peskov, N.V., *Russ. J. Phys. Chem. A,* 2008, vol. 82, no. 6, p. 951.
24. Dzis'ko, V.A., Karnaukhov, A.P., and Tarasova, D.V., *Fiziko-khimicheskie osnovy sinteza okisnykh katalizatorov* (Physicochemical Foundations of the Synthesis of Oxide Catalysts), Novosibirsk: Nauka, 1978.
25. Kheifets, L.I. and Neimark, A.V., *Mnogofaznye protsessy v poristykh sredakh* (Multiphase Processes in Porous Media), Moscow: Khimiya, 1982.
26. Chu, W., Xu, J., Hong, J., Lin, T., and Khodakov, A., *Catal. Today,* 2015, vol. 256, p. 41.
27. Guo, P., Saw, W., Eyk, P., Ashman, P., Nathan, G., and Stechel, E., *Energy Procedia,* 2015, vol. 69, p. 1770.
28. Prieto, G., Concepción, P., Murciano, R., and Martínez, A., *J. Catal.,* 2013, vol. 302, p. 37.
29. Tsubaki, N., Sun, S., and Fujimoto, K., *J. Catal.,* 2001, vol. 199, p. 236.
30. Chu, W., Chernavskii, P.A., Gengembre, L., Pankina, G.A., Fongarland, P., and Khodakov, A.Y., *J. Catal.,* 2007, vol. 252, p. 215.
31. Girardon, J.-S., Quinet, E., Griboval-Constant, A., Chernavskii, P.A., Gengembre, L., and Khodakov, A.Y., *J. Catal.,* 2007, vol. 248, p. 143.
32. Beer, M., Kunene, A., Nabaho, D., Claeys, M., and Steen, E., *J. South Afr. Inst. Min. Metall.,* 2014, vol. 114, no. 2, p. 157.
33. París, L., Lopez, J., Barrientos, F., and Pardo, M., in *Catalysis,* vol. 27, Spivey, J.J., Han, Y.-F., and Dooley, K.M., Eds., Cambridge: R. Soc. Chem., 2015, ch. 3, p. 62.
34. Jahangiri, H., Bennett, J., Mahjoubi, P., Wilson, K., and Gu, S., *Catal. Sci. Technol.,* 2014, vol. 4, p. 2210.
35. Johnson, G.R. and Bell, A.T., *ACS Catal.,* 2016, vol. 6, p. 100.
36. Zhang, Y., Nagamori, S., Hinchiranan, S., Vitidsant, T., and Tsubaki, N., *Energy Fuels,* 2006, vol. 20, p. 417.
37. Pei, Y., Ding, Y., Zhu, H., Zang, J., Song, X., Dongm, W., Wang, T., and Lu, Y., *Catal. Lett.,* 2014, vol. 144, p. 1433.
38. Peng, X., Cheng, K., Kang, J., Gu, B., Yu, X., Zhang, Q., and Wang, Y., *Angew. Chem.,* 2015, vol. 127, p. 4636.
39. Sedran, U.A. and Figoli, N.S., *Appl. Catal.,* 1985, vol.19, p. 317.
40. Kruse, N., Machoke, A.G., Schwieger, W., and Guttel, R., *ChemCatChem,* 2015, vol. 7, p. 1018.

Translated by V. Makhlyarchuk